Agbele *et al.*: Nigerian Journal of Materials Science and Engineering. Vol. 13(1): 12 - 19 (2023)

Experimental and Computational Studies of *Terminalia Catappa* Exudate and its Corrosion Inhibition Potential for Improvised Implant for Medical Application

[1*]Agbele I. E., [2]Omoniyi I. K., [2]Uba S., [2]Nwokem, N. E. and [3]Emmanuel, E. G

[1]Department of Science Laboratory Technology, Nigerian institute of Leather and Science Technology, PMB 1034, Zaria.
[2]Department of Chemistry, Ahmadu Bello University, Zaria.
[3]Department of Veterinary Medicine, Ahmadu Bello University.
*Corresponding Author E-mail: agbeleid2022@gmail.com

Abstract
Conventional weight loss and thermometric have investigated the inhibitory efficiency of Terminalia catappa on the corrosion of improvised metallic implants. The improvised metallic implant from the fan guard can be employed as a short-time profile implant item for the purpose of implantation and fixation in animals after a comparative study with the standard stainless steel. The GS-MS elucidation of chemical structures indicated the presence of phytochemical constituents responsible for TC's inhibitory capacity. The inhibition efficiency increases with increasing the inhibitor concentration; an implied phenomenon of physical adsorption was proposed for the inhibition of TC. Also, the process followed the Langmuir adsorption isotherm with very high negative values of the free energy of adsorption. Both the weight loss and thermometric results are in excellent agreement with each other. Quantum chemical parameters associated with the electronic structures of specific components of the exudate supported their inhibiting potentials.

Keywords: *Terminalia catappa*, inhibition efficiency, improvised, implant, weight loss, thermometric.

1.0 Introduction

Metallic implants play a crucial role in modern medicine, aiding in bone fixation, enhancement, and rehabilitation through implantation procedures (Zhou *et al*., 2021). Their desirable mechanical properties, biocompatibility, and historical success have made them the mainstay for a variety of orthopaedic applications. However, the long-term functionality and safety of these implants can be significantly compromised by a major adversary—corrosion.

Corrosion, the deterioration of a metal due to its interaction with its environment, presents a significant challenge in the field of metallic implants (Souza *et al*., 2020). The human body, with its presence of electrolytes and various biological fluids, creates a prime environment for this destructive process to occur. The continuous exposure of metallic implants to these aggressive fluids, such as salts, acids, and alkalis, can lead to a detrimental cascade of events.

The primary concern with corrosion in implants is the gradual loss of structural integrity and functionality. This weakening can lead to implant failure, necessitating revision surgery, which carries additional risks and costs for patients (Hrabčáková & Mašlejová, 2017; Yilmaz *et al*., 2020). Furthermore, the corrosion process can lead to the release of metal ions into the surrounding tissues, potentially triggering adverse biological responses and jeopardising long-term biocompatibility (Suhasaria *et al*., 2020).

Traditionally, various methods have been employed to mitigate corrosion in metallic implants, including painting, anodic/cathodic protection, oiling, electroplating, and the use of corrosion inhibitors (Zhou *et al*., 2021). However, these techniques often come with limitations, such as potential toxicity, environmental concerns, or limited effectiveness.

In recent years, there has been a growing interest in exploring more eco-friendly and biocompatible approaches to corrosion inhibition. Organic corrosion inhibitors, derived from natural sources, offer a promising alternative. Their advantages include being generally non-toxic, readily available, biodegradable, and often cost-effective (Awe *et al*., 2015). Additionally, the presence of specific functional groups within these organic molecules allows them to effectively adsorb onto the metal surface, forming a protective barrier that hinders the corrosion process (Yilmaz *et al*., 2020).

The current study focuses on investigating the potential of *Terminalia catappa* exudate, a natural extract from the *Combretaceae* family plant, as a corrosion inhibitor for

metallic implants in a simulated physiological environment (1 M HCl solution). This plant extract is known to possess various beneficial properties, including anti-parasitic, anti-bacterial, and anti-fungal activities, suggesting its potential biocompatibility (Prasad *et al*., 2017). Exploring the effectiveness and mechanism of this natural extract on corrosion inhibition could pave the way for the development of safer and more sustainable strategies to enhance the longevity and safety of metallic implants used in the medical field.

2.1 Collection of plant latex and preparation of plant extract

Plant exudate of *Terminalia catappa* was dissolved in a 500ml solution of ethanol for 48 hours. Sequentially, sufficient exudate was added to the ethanol according to the method described in Dash *et al*., 2005. The samples were filtered using Whatman filter paper No. 1. The filtrate was further subjected to evaporation by a rotatory evaporator at 358K to avoid ethanol contaminant. The stock solution of the extract was prepared in different concentrations of the extract by dissolving 1.0 to 5.0g of the extract in 1L of 1MHCl acid respectively

2.2 Phytochemical Analysis on TC

Phytochemical analysis of the ethanol was carried out according to the method reported by Eddy *et al*., 2018. This was essential for the identification of bioactive components of the plant and the present of organic matter. These compounds have potential corrosion inhibitors for many metals in an acidic medium.

2.3 Preparation of specimen

The specimens were cut using a saw into the required dimension 2x1x0.5cm then descaled by brushing with an emery paper. The oil was removed with ethanol and dried with acetone, then stored in desiccators for further use.

2.4 Comparative studies of the standard stainless and improvised metallic implants from the fan guard

2.4.1 The mechanical properties of metallic implant

The destructive test was achieved using Hounsfield Tensometer serial no W3179 (made in England) at Mechanical Engineering at Ahmadu Bello University. Mechanical properties are physical properties that a material exhibits upon the application of forces. Properties are the modulus of elasticity, ultimate tensile strength, force, elongation, hardness, and fatigue limit (Farabi *et al*., 2010).

2.4.2 The chemical properties of metallic implant

The chemical composition of metallic implants employed for the study is examined using the Handheld NITON Metal Analyzer Model: XL_2800 X-ray Fluorescence Spectrometers (XRF) at the Mechanical Engineering Department of Ahmadu Bello University Zaria (Gepreel and Niinomi, 2013; Souza *et al*., 2020; Yilmaz *et al*., 2020).

2.5 Gas chromatography mass spectrometery (GC-MS)

GC-MS analysis of the plant ethanol extract of *Terminalia catappa* was performed using a Perkin-Elmer GC Clarus 500 system comprising an AOC-20i auto-sampler and a gas chromatograph interfaced to a mass spectrometer (GC-MS). GC-MS analysis will be carried out on gas chromatograph interfaced with a mass spectrometer (GC-MS) instrument. Interpretation on mass spectrum GC-MS were conducted using the database of National Institute Standard and Technology (NIST). The name, molecular weight, and structure of the components of the test materials of the inhibitors were ascertained and the concentrations of the identified compounds were determined through area and height normalization (Pasdaran *et al*., 2013).

2.6 Corrosion study

2.6.1 Weight loss

The corrosion rates of the implant were calculated by considering the total affected sample area and immersion time in a 250 mL conical flask containing 1.0M HCl of the acid at pH 3, the corrodent in the absence and presence of varying concentrations of the studied exudate (0.1 – 0.5 g/ L) at temperatures 303–333 K maintained in a thermostat water bath. After every 24 hours, the corrosion product is removed by washing each coupon (withdrawn from the test solution) in a solution containing 50 % NaOH and 100 g l^{-1} of zinc dust. The washed coupon was rinsed in acetone and dried in the air before re-weighing. The difference in weight for 168 hours was taken as total weight loss, the experiments were carried out in triplicate to get good results. From the average weight loss results, the percentage of inhibition efficiency (% IE) and the degree of surface coverage (θ) was calculated using the following equations (Ameh, 2018).

$$I\,(\%) = \left(1 - \frac{W_1}{W_2}\right) \times 100 \quad (1)$$

$$\theta = \left(1 - \frac{W_1}{W_2}\right) \quad (2)$$

Where W_1 and W_2 are the average weight losses (g/dm^3) for mild steel or aluminum in the presence and absence of inhibitor in HCl or H_2SO_4 solution respectively

The corrosion rates (in g m^{-2} h^{-1}) for stainless steel implant or improvised implant corrosion in different

concentrations of the studied exudate determined for 168 h immersion period from weight loss using equation 3

$$Corrosion\ rate = \frac{534W}{DAT} \quad 3$$

where W = weight loss (mg); D = density of specimen (g/cm^3), A = area of specimen (square inches) and T = period of immersion (hour).

2.6.2 Thermometric method

The thermometric experiment was carried out as reported elsewhere (Ameh *et al*., 2012). The volume of the corrodent used is 50 ml while the initial temperature in all the experiments is maintained at 303 K. The reaction number (RN) of each system is calculated by dividing the difference between the highest and lowest temperature attained by the time interval as expressed in equation 4.

$$\text{RN } (^{o}\text{Cmin}^{-1}) = \frac{T_f - T_i}{t} \quad 4$$

where T_f and T_i are the final and initial temperatures and t is the time interval. From the reaction number, the inhibition efficiency (% I) of the inhibitor will be calculated by using the following equation 5

$$\%I = \frac{RN_{aq} - RN_{wi}}{RN_{aq}} \quad 5$$

Where RN_{aq} is the reaction number in the absence of inhibitors (blank solution) and RN_{wi} is the reaction number of 0.1 M HCl containing the studied inhibitor.

2.7 Quantum chemical calculations

The use of quantum chemical methods to calculate electronic properties is possibly relevant to explain the inhibiting action. The viability of inhibitor molecules to donate or accept electrons can be predicted with analysis of global reactivity parameters, such as the energy gap (ΔE) between the Highest Occupied Molecular Orbital (HOMO) and Lowest Unoccupied Molecular orbital (LUMO) (Madkour *et al*., 2018; Zakaria *et al*., 2022).

3.0 Results and Discussion

3.1 Phytochemical screening

The phytochemical constituents of TC exudate are presented in Table 1. The plant exudates were screened for the presence/absence of secondary phytochemical metabolites using the standard qualitative phytochemical methods. The presence of these compounds enhances the inhibition of improvised implants in hydrochloric acid solution. The phyto-constituents in TC are listed in Table 1.

The results of the improvised metallic implant sourced from waste electrical fan-guard compared with the standard stainless-steel implant based on mechanical and chemical properties as presented in Table 2. The biocompatibility choice of any implant for medical purposes is dependent on the mechanical properties such as young modulus was determined to be 915.6 and 1757, and ultimate tensile stress obtained was 820.41 and 931.37 for improvised implant and standard stainless steel respectively. The improvised metallic implant sample from the fan guard has lower ultimate tensile strength and Young modulus higher than that of the standard steel; this implies that the improvised sample can withstand corrosion medium longer than the standard stainless steel (Li *et al*., 2020).

Table 1: Phytochemical Screening of TC exudate using GC-MS

S/N	Chemical constituent	Inference/Observation
1	Tannins	+
2	Flavonoid	+
3	Alkaloid	+
4	Saponins	-
5	Carbohydrate	-
6	Anthraquinone	+
7	Steroid	+

Figure 1 revealed the X-ray diffraction (XRD) analyses, which is a nondestructive technique that provides detailed information about the crystallographic structure, chemical composition, and physical properties of the material (Pandey *et al.*, 2021).

A chemically compatible metallic material should not trigger adverse tissue reactions through the use of inert alloy as selected components only. Also, it must possess enough potency to form protective passive layers, limiting the release of metal ions into the environment (Presuel *et al*., 2008). Biocompatibility is the rejection of elemental components that are toxic or elements that can cause allergic problems such as Ni, Co, and V, while the best candidates are Ti, Nb, Zr, and Ta (Niinomi, 2002). Cobalt provides a continuous phase for basic properties as reported by Shen *et al* (2021). Chromium provides corrosion resistance through the oxide surface. Molybdenum provides strength and bulk corrosion resistance (Sinnett-Jones *et al*., 2005). Nickel and carbon enhance mechanical properties such as ductility. Therefore, an elemental component is critical in the determination of the biocompatibility of implants as reported by (Jadhav *et al*., 2018). Therefore, the improvised metallic implant from fan guard can be employed as a short time profile implant items for the purpose of implantation and fixation in animals.

3.2 Effect of time at 303K on the corrosion rate of the improvised metallic implant using TC as an inhibitor

The corrosion rate of the improvised metallic implant in 1.0 M HCl solution has direct relation with immersion time but inversely relates to the inhibitor concentrations in a corrosion system (Nady *et al*., 2021). Figure 2A present the graph of weight loss against immersion time using TC as inhibitor. The weight loss of the improvised metallic implant decreased with an increase in inhibitor concentrations but increased with immersion time, at the same time, the highest weight loss was observed at the lowest inhibitor concentration of 0.1 g/L in an acid medium.

Table 2: Mechanical and chemical properties of improvised metal and standard stainless implants

Parameters	Force (N)	UTS (N/m^2)	Surface Area (m^2)	Strain	Young modulus	Elongation (%)
Standard	2375	931.37	2.55	0.57	1757.3	57
Improvised	1450	820.41	1.767	0.896	915.6	89.60
Elemental composition	Standard %	Fe (93.9)	Zn (4.27)	Zr (0.32)	Nb (1.69)	Pb (0.25
	Improvised%	Fe (97.9)	Zn (1.31)	Zr (0.08)		

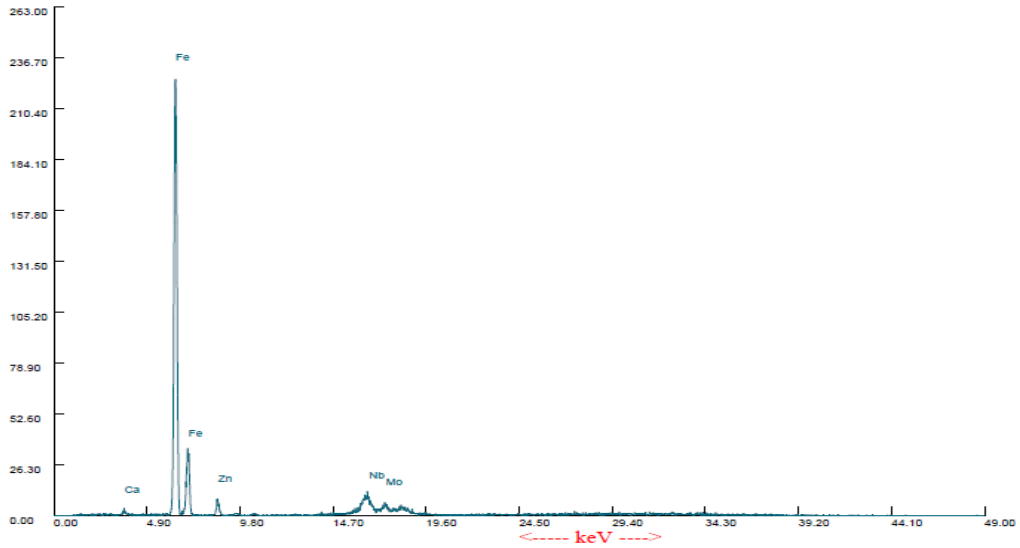

A

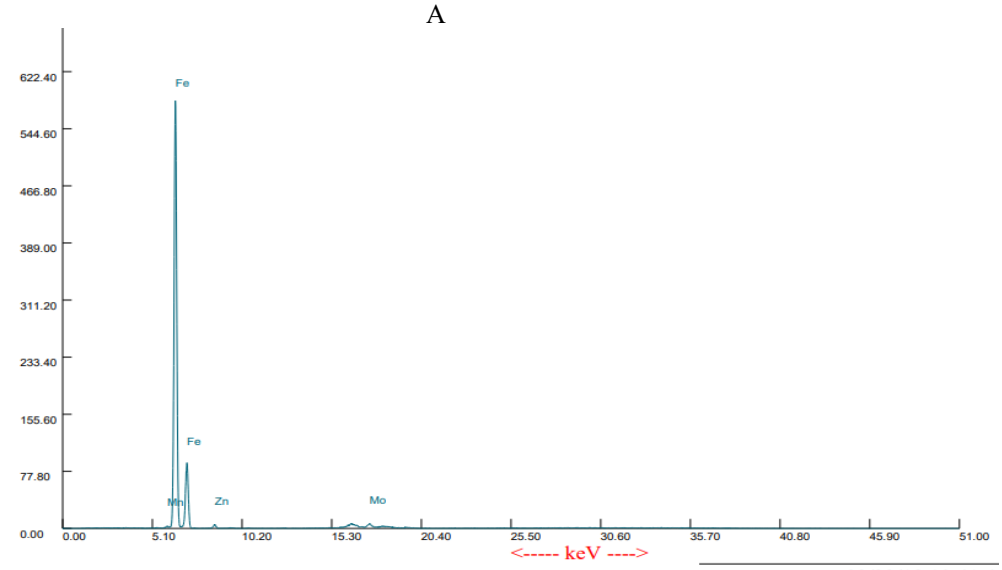

B

Figure 1: Comparative study of spectra of the standard stainless-steel SI (A) and the improvised metallic implant IM (B) using X-Ray diffraction

Table 3: Deduced data for the corrosion rate, surface coverage, inhibition efficiency, enthalpy, and entropy obtained from the weight lost method for the improvised steel implant

Conc of inhibitor (g/l)	Corrosion rate (mm/yr)	Surface coverage (θ)	Inhibition efficiency (%) IE)	ΔH ($Kjmol^{-1}$)	ΔS ($Kjmol^{-1}$)
Blank	0.3091			26.53	-0.2
0.1	0.117787	0.6190	61.90	38.33	-0.16
0.2	0.08834	0.7143	71.43	46.17	-0.14
0.3	0.058894	0.8095	80.95	52.29	-0.12
0.4	0.052081	0.8261	82.61	55.12	-0.12
0.5	0.0500	0.8326	83.26	63.35	-0.09

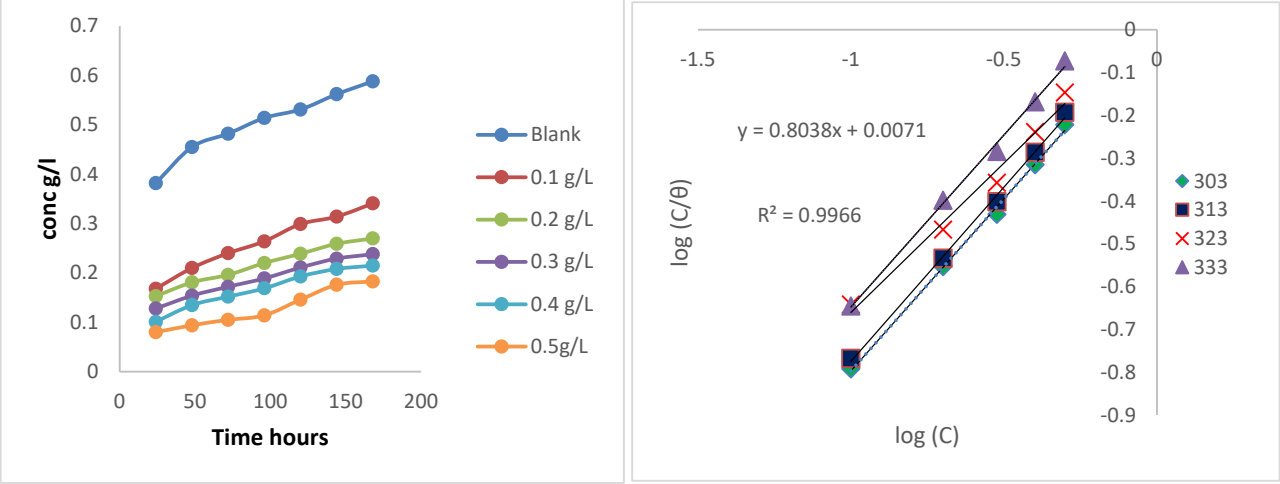

A B

Fig. 2: A: Variation of weight loss with time for the corrosion of the improvised steel in 1M HCl containing TC at 303 K and B Langmuir isotherm at 303K.

Further, the highest corrosion resistance (inhibition efficiency) was observed when the inhibitor concentration was 0.5 g/L at the lowest temperature of 303K. This is similar to the work of Adeniji and Akindehinde (2018); Awe, (2019); Eddy *et al*. (2018). This is an indication that the inhibitors are adsorbed on the surface of metallic implants. Therefore, the adsorption of inhibitors reduced the available surface area on metal surfaces against corrosion by the geometric blocking effect (Alvarez *et al.*, 2018; Brycki *et al*., 2018; Saha *et al*., 2016). The following researchers reported similar trends (Ameh, 2018; Awe, 2019; Eddy *et al*., 2018; Umoren, *et al*., 2011; Odiongenyi *et al*., 2009).

3.3 Entropy and enthalpy changes of corrosion inhibition process

The values of enthalpy change ΔH and entropy change ΔS obtained at different immersion times are also given in Table 3. The entropy of activation in the presence and absence of the inhibitors used in this study has negative values, which indicate that the activated complex in the rate-determining step represents an association rather than dissociation, therefore there was a decrease in disordering from the reactant to the activated complex (Kosari *et al*., 2014; Lebrini *et al*., 2010). A negative value of the enthalpy of activation obtained means that the process is exothermic, and it needs less energy to achieve the activated state (Kaur *et al*., 2019).

3.4 Thermodynamic/adsorption study

The degree of surface coverage at various concentrations of the plant exudates at the temperature 303K was tested with the Langmuir isotherm equation. Table 4 shows the parameter for Langmuir isotherm. It is also significant to note that the value of the adsorption equilibrium constant obtained from the intercept of each adsorption isotherm is related to the free energy of adsorption according to the equation.

$$\Delta G^{o}_{ads} = -2.303RTlog(55.5b_{ads}) \qquad 6$$

Table 4: Langmuir parameters for the adsorption of *terminalia catappa* (TC).

Temperature K	Slope	log b_{ads}	ΔG^0 ads(kJ/mol)	R^2
303	0.8038	0.0071	-10.16	0.99

From Table 4, the result revealed that the adsorption mechanism of TC onto the metal implant surface obeys Langmuir isotherm at the studied temperature and time, due to high values of R^2 obtained [and] the slope is close to unity. This implies that there is a strong adherence to Langmuir adsorption isotherm. This implies monolayer coverage and homogenous distribution of the TC on the surface of the metal, as predicted by the Langmuir equation (Chen *et al*., 2022; Yang *et al*., 2020).

3.5 Thermometric method

Thermometric measurement of plant exudate on the corrosion of metallic implant in Table 5, revealed that the values of reaction number decreased in the presence of TC exudate compared to the blank solution. The inhibition efficiency as expected increased with an increase in concentration of the inhibitor, which supports our findings from the previous weight loss study. Results obtained from thermometric and gravimetric methods at 303 K were in excellent agreement as can be seen in high values of Pearson product-moment correlation 'r' which is 0.987126362 in Table 6. The observed difference in the values of inhibition efficiencies obtained from the gravimetric and thermometric methods may be attributed to the difference in the time of inhibitors to form an adsorbed layer on the improvised metallic implant surface that inhibits corrosion. Also, the weight loss method measures average value over a longer time while the thermometric method is an instantaneous measurement at a shorter period. The result in Table 6 showed that there was great agreement between the two corrosion monitoring methods as the Pearson product-moment correlation (r) value close to 1 Puth *et al*. (2014). Table 7 showed that adsorption of the inhibitor might have proceeded through these ten groups. From the analysis of GCMS the following inference were made 3h-indole, 2 methyl-7-phenylindole, 2-ethylacridine, Methyl-1-adamantaneacetamide, Benzo(h)quinoline, thymol, quinone, 1, 4- bis (trimethylsilyl) benzene and 1,2-bis(trimethylsilyl) benzene. The value of E_{HOMO} increased in the following order: 3h-indole > 2 methyl-7-phenylindole > 2-ethylacridine > Methyl-1-adamantaneacetamide > Benzo(h)quinoline > thymol > quinone, 1, 4- bis (trimethylsilyl) benzene > 1,2-bis(trimethylsilyl) benzene. The values of E_{HOMO} obtained also indicate the greater tendency of these phytochemical constituents to donate the electron to the vacant d-orbital of the iron atom, therefore TC can be said to have the tendency to bind with it.

Table 5: Thermometric results for *tterminalia catappa*

C(g/L)	Initial temperature	Max temperature	Reaction number	Percent inhibition
Blank	30	32.6	0.52	-
BSF	30	31.0765	0.2153	58.89
0.1	30	30.923	0.1846	64.5
0.2	30	30.6525	0.1305	74.9
0.3	30	30.442	0.0884	83.46
0.4	30	30.3715	0.0743	85.72
0.5	30	30.2825	0.0565	89.14

Table 6: Pearson product-moment correlation of gravimetric and thermometric methods

	Gravimetric TC (303K)	Thermometric TC (303K)
Gravimetric	1	
Thermometric	0.987126362	1

Quantum chemical calculations

Table 7: Frontier molecular orbital energies of active constituents of ethanol extract of plants

Constituents	Molecular weight	HOMO	LUMO	Energy gap/ LUMO-HOMO
1, 4- bis (trimethylsilyl) benzene	222.48	-915.86	23.45	939.31
1,2-benzisothiazol-3-amine	150.205	-828.46	-74.21	754.25
quinone	129.162	-891.60	-62.44	954.04
1,2-bis(trimethylsilyl) benzene	222.48	-916.29	31.99	948.28
3h-indole	117.151	-630.12	-122.08	508.04
2 methyl-7-phenylindole	207.276	-803.87	-6.95	810.82
2-ethylacridine	207.276	-825.17	-113.83	711.34
Methyl-1-adamantaneacetamide	207.317	-851.13	88.07	939.2
thymol	150.221	-864.98	27.56	892.54
Benzo(h)quinoline	179.22	-856.65	-67.06	789.59

metallic implant surface, the results obtained are in agreement Ameh, (2018), Lin *et al*., (2021), and Miar *et al*., (2021). It has also been found that the inhibition capacities of most corrosion inhibitors are strongly dependent on some molecular and electronic parameters of the inhibitors (Eddy *et al*., 2015)

Conclusion

All the phytochemical constituents in TC exudate act as an efficient corrosion inhibitor for improvised metallic implants in HCl acid solution and their inhibitory efficacy increases with an increase in concentration of the TC with maximum efficiency obtained at 0.5g/l. The results of GCMS all indicate the corrosion reaction was inhibited by the adsorption of the organic matter onto the corroding steel surface. Analysis suggests the mechanism involves the adsorption of organic materials from the extract onto the metal, creating a barrier against corrosive agents. The study proposes these TC-incorporated implants as potential short-term solutions for animal models. However, further research is needed to understand the specific components responsible and ensure long-term biocompatibility. Overall, this study highlights a promising green approach for corrosion protection of metallic implants in medical applications.

References

Adeniji, S. E., and Akindehinde, B. A. (2018). Comparative analysis of adsorption and corrosion inhibitive properties of ethanol extract of Dialium Guineense leaves for mild steel in 0.5 M HCl. *Journal of Electrochemical Science and Engineering*, *8*(3), 219–226.

Alvarez, P. E., Fiori-Bimbi, M. V., Neske, A., Brandan, S. A., and Gervasi, C. A. (2018). Rollinia occidentalis extract as green corrosion inhibitor for carbon steel in HCl solution. *Journal of Industrial and Engineering Chemistry*, *58*, 92–99.

Ameh, P. O. (2018). Electrochemical and computational study of gum exudates from Canarium schweinfurthii as green corrosion inhibitor for mild steel in HCl solution. *Journal of Taibah University for Science*, *12*(6), 783–795.

Awe, F. E. (2019). Adsorptive studies of the inhibitive properties of ethanolic extracts of Parinari polyandra on mild steel in acidic media. *Communication in Physical Sciences*, *4*.

Brycki, B., Kowalczyk, I. H., Szulc, A., Kaczerewska, O., and Pakiet, M. (2018). Organic corrosion inhibitors. *Corrosion Inhibitors, Principles and Recent Applications*, *3*, 33.

Chen, X., Hossain, M. F., Duan, C., Lu, J., Tsang, Y. F., Islam, M. S., and Zhou, Y. (2022). Isotherm models for adsorption of heavy metals from water-a review. *Chemosphere*, 135545.

Eddy, N. O., Ameh, P. O., and Essien, N. B. (2018). Experimental and computational chemistry studies on the inhibition of aluminium and mild steel in 0.1 M HCl by 3-nitrobenzoic acid. *Journal of Taibah University for Science*, *12*(5), 545–556.

Gepreel, M. A.-H., and Niinomi, M. (2013). Biocompatibility of Ti-alloys for long-term implantation. *Journal of the Mechanical Behavior of Biomedical Materials*, *20*, 407–415.

Hrabčáková, L., and Mašlejová, A. (2017). Metallographic Analysis of Filiform Corrosion. *Solid State Phenomena*, *270*, 142–146.

Jadhav, K., Rajeshwari, H. R., Deshpande, S., Jagwani, S., Dhamecha, D., Jalalpure, S., Subburayan, K., and Baheti, D. (2018). Phytosynthesis of gold nanoparticles: characterization, biocompatibility, and evaluation of its osteoinductive potential for application in implant dentistry. *Materials Science and Engineering: C*, *93*, 664–670.

Kaur, B., Gupta, R. K., and Bhunia, H. (2019). Microporous and Mesoporous Materials Chemically activated nanoporous carbon adsorbents from waste plastic for CO 2 capture : Breakthrough adsorption study. *Microporous and Mesoporous Materials*, *282*(March), 146–158. https://doi.org/10.1016/j.micromeso.2019.03.025

Kosari, A., Moayed, M. H., Davoodi, A., Parvizi, R., Momeni, M., Eshghi, H., and Moradi, H. (2014). Electrochemical and quantum chemical assessment of two organic compounds from pyridine derivatives as corrosion inhibitors for mild steel in HCl solution under stagnant condition and hydrodynamic flow. *Corrosion Science*, *78*, 138–150.

Lebrini, M., Robert, F., and Roos, C. (2010). Inhibition effect of alkaloids extract from Annona squamosa plant on the corrosion of C38 steel in normal hydrochloric acid medium. *International Journal of Electrochemical Science*, *5*(11), 1698–1712.

Li, Z., Jin, Z., Xu, X., Zhao, T., Wang, P., and Li, Z. (2020). Combined application of novel electromagnetic sensors and acoustic emission apparatus to monitor corrosion process of reinforced bars in concrete. *Construction and Building Materials*, *245*, 118472. https://doi.org/10.1016/j.conbuildmat.2020.118472

Lin, H.-Y., Chen, C.-Y., Lin, T.-C., Yeh, L.-F., Hsieh, W.-C., Gao, S., Burnouf, P.-A., Chen, B.-M., Hsieh, T.-J., Dashnyam, P., and others. (2021). Entropy-driven binding of gut bacterial $β$-glucuronidase inhibitors ameliorates irinotecan-induced toxicity. *Communications Biology*, *4*(1), 1–10.

Madkour, L. H., Kaya, S., Guo, L., and Kaya, C. (2018). Quantum chemical calculations, molecular dynamic

(MD) simulations and experimental studies of using some azo dyes as corrosion inhibitors for iron. Part 2: Bis--azo dye derivatives. *Journal of Molecular Structure*, *1163*, 397–417.

Miar, M., Shiroudi, A., Pourshamsian, K., Oliaey, A. R., and Hatamjafari, F. (2021). Theoretical investigations on the HOMO--LUMO gap and global reactivity descriptor studies, natural bond orbital, and nucleus-independent chemical shifts analyses of 3-phenylbenzo [d] thiazole-2 (3 H)-imine and its para-substituted derivatives: Solvent and. *Journal of Chemical Research*, *45*(1–2), 147–158.

Nady, H., El-Rabiei, M. M., Bahrawy, A., and El-Katori, E. E. (2021). Assessment of H2O2/albumin and glucose on the biomedical iron alloys corrosion in simulated body fluid: Experimental, surface, and computational investigations. *Journal of Molecular Liquids*, *339*, 116823.

Niinomi, M. (2002). Recent metallic materials for biomedical applications. *Metallurgical and Materials Transactions A*, *33*(3), 477–486.

Obot, I. B., Umoren, S. A., and Obi-Egbedi, N. O. (2011). Corrosion inhibition and adsorption behaviour for aluminuim by extract of Aningeria robusta in HCl solution: Synergistic effect of iodide ions. *Journal of Materials and Environmental Science*, *2*(1), 60–71.

Odiongenyi, A. O., Odoemelam, S. A., and Eddy, N. O. (2009). Corrosion inhibition and adsorption properties of ethanol extract of Vernonia amygdalina for the corrosion of mild steel in H2SO4. *Portugaliae Electrochimica Acta*, *27*(1), 33–45.

Pandey, A., Dalal, S., Dutta, S., and Dixit, A. (2021). Structural characterization of polycrystalline thin films by X-ray diffraction techniques. *Journal of Materials Science: Materials in Electronics*, *32*(2), 1341–1368.

Prasad, K., Bazaka, O., Chua, M., Rochford, M., Fedrick, L., Spoor, J., Symes, R., Tieppo, M., Collins, C., Cao, A., and others. (2017). Metallic biomaterials: Current challenges and opportunities. *Materials*, *10*(8), 884.

Presuel-Moreno, F., Jakab, M. A., Tailleart, N., Goldman, M., and Scully, J. R. (2008). Corrosion-resistant metallic coatings. *Materials Today*, *11*(10), 14–23.

Saha, S. K., Dutta, A., Ghosh, P., Sukul, D., and Banerjee, P. (2016). Novel Schiff-base molecules as efficient corrosion inhibitors for mild steel surface in 1 M HCl medium: experimental and theoretical approach. *Physical Chemistry Chemical Physics*, *18*(27), 17898–17911.

Shen, Y., Xue, H., Wang, S., Wang, Z., Zhang, D., Yin, D., Wang, L., and Cheng, Y. (2021). A highly promising high-nickel low-cobalt lithium layered oxide cathode material for high-performance lithium-ion batteries. *Journal of Colloid and Interface Science*, *597*, 334–344.

Sinnett-Jones, P. E., Wharton, J. A., and Wood, R. J. K. (2005). Micro-abrasion--corrosion of a CoCrMo alloy in simulated artificial hip joint environments. *Wear*, *259*(7–12), 898–909.

Souza, J. C. M., Apaza-Bedoya, K., Benfatti, C. A. M., Silva, F. S., and Henriques, B. (2020). A comprehensive review on the corrosion pathways of titanium dental implants and their biological adverse effects. *Metals*, *10*(9), 1272.

Suhasaria, A., Murmu, M., Satpati, S., Banerjee, P., and Sukul, D. (2020). Bis-benzothiazoles as efficient corrosion inhibitors for mild steel in aqueous HCl: molecular structure-reactivity correlation study. *Journal of Molecular Liquids*, *313*, 113537.

Vinogradov, A., Vasilev, E., Kopylov, V. I., Linderov, M., Brileves2ky, A., and Merson, D. (2019). High performance fine-grained biodegradable Mg-Zn-Ca alloys processed by severe plastic deformation. *Metals*, *9*(2), 186.

Yang, Y., Koh, K. Y., Li, R., Zhang, H., Yan, Y., and Chen, J. P. (2020). An innovative lanthanum carbonate grafted microfibrous composite for phosphate adsorption in wastewater. *Journal of Hazardous Materials*, *392*, 121952.

Yilmaz, B., Pazarceviren, A. E., Tezcaner, A., and Evis, Z. (2020). Historical development of simulat
.ed body fluids used in biomedical applications: A review. *Microchemical Journal*, *155*(February), 104713. https://doi.org/10.1016/j.microc.2020.104713

Zakaria, K., Abbas, M. A., and Bedair, M. A. (2022). Herbal expired drug bearing glycosides and polysaccharides moieties as green and cost-effective oilfield corrosion inhibitor: Electrochemical and computational studies. *Journal of Molecular Liquids*, *352*, 118689.

Zhou, H., Liang, B., Jiang, H., Deng, Z., and Yu, K. (2021). Magnesium-based biomaterials as emerging agents for bone repair and regeneration: from mechanism to application. *Journal of Magnesium and Alloys*, *9*(3), 779–804. https://doi.org/10.1016/j.jma.2021.03.004